Spatter Rate Estimation in the Short-Circuit Transfer Region of GMAW

A study shows the optimal model for estimating spatter rate using an artificial neural network in the short circuit transfer region of GMAW

BY M. J. KANG, Y. KIM, S. AHN, AND S. RHEE

ABSTRACT. This study was conducted to develop the best model to estimate spatter rate for the short circuiting transfer mode of the gas metal arc (GMA) welding process. Utilizing an artificial neural network. The spatter rate generated during welding is a barometer of process stability for metal transfer, and it depends on the periodic waveforms of the welding current and arc voltage in the short circuiting mode. Twelve factors representing the characteristics of the waveforms as inputs and the spatter rate as an output were employed as variables for the neural network. Two neural network models were evaluated for estimating the spatter rate: one model did not consider arc extinction; the other model did. The input vector and the nodes of hidden layers for each model were optimized to provide an adequate fit, and estimated performance of each optimized model to the spatter rate was assessed and compared with the previously proposed model. It was, in addition, demonstrated in this study that the combined neural network model was more effective in predicting the spatter rate than other models through evaluation of the estimated performance of each optimized model.

Introduction

In GMA welding, process quality can be represented by bead shape, implying the bead width and penetration depth, or by spatter rate. Prediction models to estimate process quality in terms of quantity, nevertheless, are required since the quantities cannot be measured during a welding process. The short circuiting transfer mode has periodic characteristics of arc and short circuit between the welding wire and the weld pool. The metal droplet grows at the electrode tip when the arc is maintained, and it is transferred to the weld pool while in contact with the tip. Irregular waveforms of the welding current and arc voltage indicate variations in the metal droplet size and imbalance between several forces on the droplet. The likelihood of spatter generated, therefore, is significantly greater when the short-circuit time or arc time is irregular (Ref. 1) with the spatter rate closely related to the regularity of the arc and short-circuit time. A stable arc leads to a low spatter rate and regular waveform while an unstable arc causes a high spatter rate. An evaluation of the arc state through correlation analysis between the standard deviation of arc time and stability was attempted for the the short circuiting transfer mode (Ref. 2). It was also reported that the short circuit peak current and standard deviation of the arc time affect the arc stability to a great extent (Ref. 3), and Suban (Ref. 4) has attempted to analyze weldability adopting the probability distribution function and FFT analysis of current waveform, thus showing that the arc becomes stable with higher intensity and narrow distribution. Shinoda and Nishikawa (Ref. 5) have reported that arc stability is related to the period and size of the area wherein the current-voltage diagram (I-V diagram) is drawn in the short circuiting mode. They have proposed an index expressing arc stability by adopting the welding current and the arc voltage waveforms in short circuiting transfer. Gupta (Ref. 6), in addition, has examined how wire size, gas flow rate, and electrode extensions affect the spatter loss showing that a small-sized wire has a higher spatter loss at a lower arc voltage while a large-sized wire has a higher spatter loss at a higher arc voltage with the phenomena depending on the metal transfer mode. Hermans et al. (Refs. 7, 8) showed that arc voltage and wire feed rate affect the short-circuiting frequency in GMA welding and that the arc becomes more stable as the standard deviation of the short-circuit frequency gets smaller. They have, in addition, proved that the arc stability is affected by weld pool oscillation, and the arc reaches the maximum stability state when the short-circuit frequency equals weld pool oscillation. Ogunbiyi and Norrish (Ref. 9) have classified metal transfer mode and arc stability using several indices induced from minimum current, average current, maximum current, and average voltages during the sampling period. Mita et al. (Ref. 10) have extracted the waveform elements, including arc time, short-circuit time, average arc current, and average short-circuit current, and their standard deviations, from the measured signals of the welding current and arc voltage. They have proposed several regression models composed of the waveform factors comprising the waveform elements and their standard deviations, and developed the optimal regression model based on the evaluation of welders' subjective judgment, leading to a consideration of the model as the arc stability estimation index. They have demonstrated that the arc becomes more stable as the index moves down and vice versa. Most of the results reported hitherto have been induced from the arc stability or the metal transfer mode using the regularity of the waveform factors or particular relationships between the welder's experience

*M. J. KANG is a Senior Researcher (*moojin@kitech.re.kr*), Advanced Welding and Joining Technology Team, KITECH, Chonan, Korea. Y. KIM is a Researcher (*yongjaekim@doosanheavy.com*), Welding Technology Research Team, Doosan Heavy Industries and Construction Co., Ltd., Changwon, Korea. S. AHN is an Associate Professor (*shahn@chuldo.krc.ac.kr*), Dept. of Train Operation and Mechatronics Engineering, Korea National Railroad College, Euiwang, Korea. S. RHEE is an Associate Professor (*srhee@hanyang.ac.kr*), Dept. of Mechanical Engineering, Hanyang University, Seoul, Korea.*

KEY WORDS

Gas Metal Arc Welding
Short Circuit Transfer
Neural Network
Spatter Rate
Computer Data Analysis

and certain models to estimate the arc state. The models, nevertheless, are not explained quantitatively and are deficient in statistical verification. The authors (Refs. 11, 12) have proposed a statistical model to predict the process stability quantitatively by applying a relationship between the spatter rate and the waveform factors in GMA welding to multiple regression analysis, but there is still a large error in predicting the spatter rate with these models.

If the stability of the welding process is not assessed precisely during welding, it becomes very difficult to comprehend whether welding is performed under proper conditions. The majority of spatters occur under improper welding conditions leading to an understanding that it is possible to change the process conditions to get ideal weld quality if the process state is precisely assessed, and this is dependent on the estimation accuracy of a prediction model assessing the state of the welding process.

This study attempted to develop optimal models, which can predict process stability (or metal transfer stability) for short circuit transfer in GMA welding in real time quantitatively through the use of an artificial neural network. And these neural network models can be adopted to control the arc when an improper welding condition is established or the arc status is changed by any disturbances. Ideal weld quality with minimal spatter can specifically be obtained by an appropriate adjustment of the arc voltage wherein the control performance is dependent on the estimation quality of the model. This study focuses on the development of estimation performance.

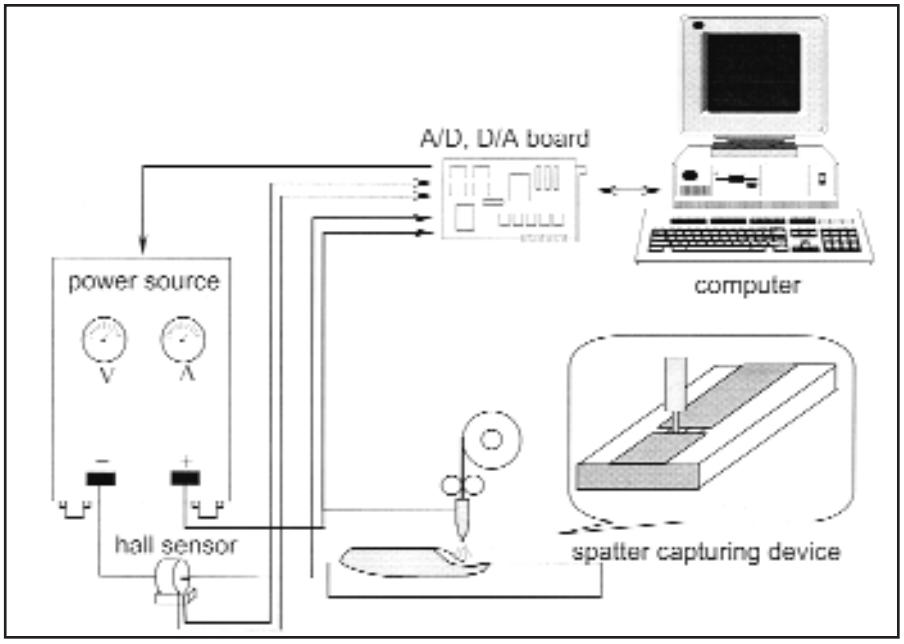

Fig. 1 — Configuration of experimental setup.

Table 1 — Welding Conditions and the Number of Experiments per Setting Condition

Wire Feed Rate (m/min)	Contact Tube-to-Workpiece Distance, CTWD (mm)	Welding Voltage (V)	No. of Welding Experiments Per Setting Condition
3.4	15	19 ~ 25	6
6.0	15	20 ~ 26	6
	20	21 ~ 27	3
	25	21 ~ 27	3
7.3	15	21 ~ 27	3
	20	22 ~ 28	4
	25	21 ~ 27	3
8.6	20	23 ~ 27	6

Experimental Procedure

The experimental devices used in this study to extract the waveform factors affecting spatter generation included a welding power source, a spatter capturing device, welding process parameter sensors, A/D and D/A converters, and a computer, as shown in Fig. 1. The welding power source used was a transistorized inverter-controlled type with a maximum output of 350 A. It had only constant voltage characteristics without any waveform control functions.

The welding current and voltage were used as set variables, and the welding current was measured with a hall sensor that was attached to the ground cable, while the arc voltage was measured from the output terminals of the welding power source. The measured signals were put into the computer through an A/D converter with a maximum sampling rate of 200 kHz.

A gathering device for spatter was made of brass and in the shape of a box. The welding gun and workpiece were completely enclosed by the device before welding to prevent the spatter from splashing out during welding. The welding experiment was conducted for one minute for each welding condition, and the spatter in the gathering device was subsequently collected and screened using a sieve with 300 (grid/in.^{2}) mesh. The spatter on the sieve was weighed using an electronic balance. The characteristics of spatter, such as the size or type, were not considered. The welding variables were 100% CO_2 shielding gas with a flow rate of 20 L/min, a 1.2-mm-diameter AWS ER70S-6 welding wire, 6-mm-thick ASTM A36M workpiece, and a welding speed of 5 mm/s.

The welding parameters are shown in Table 1. The welding conditions lacking the pure short circuit metal transfer mode (250 A and 28 V or higher) were excluded and all of the data were handled solely for the short circuit transfer mode. The welding experiments on plate without a groove were repeated five to six times under the same welding conditions to reduce experimental errors.

The sampling rate to gather the waveforms of the arc voltage and welding current was 5000 samples/s, and the waveform signals were collected 10 seconds after the welding start at 20-second intervals. A digital low-pass filter with a 200-Hz cutoff frequency removed the noise on the signals, and six waveform factors and their standard deviations influencing the spatter generation were extracted from the welding current and arc voltage waveforms. The 12 extracted factors are as follow (Fig. 2): short-circuit period (T), arc time (T_a), short-circuit time (T_s), short-circuit peak current (I_p), short-circuit in-

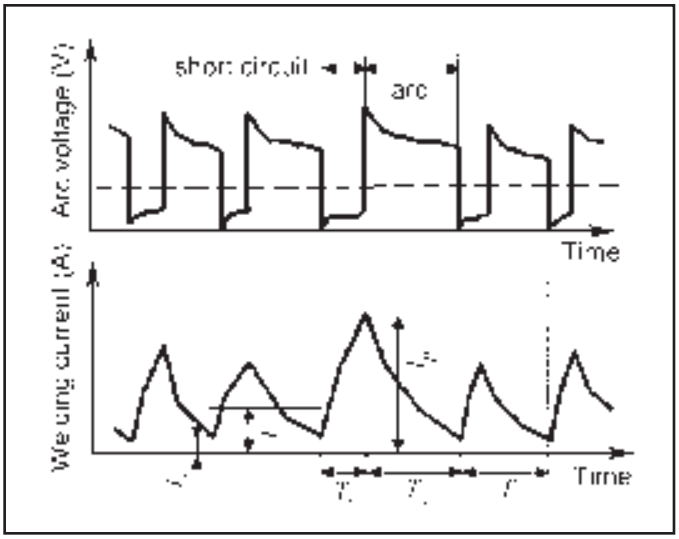

Fig. 2 — Waveforms of arc voltage and welding current in short-circuit transfer mode.

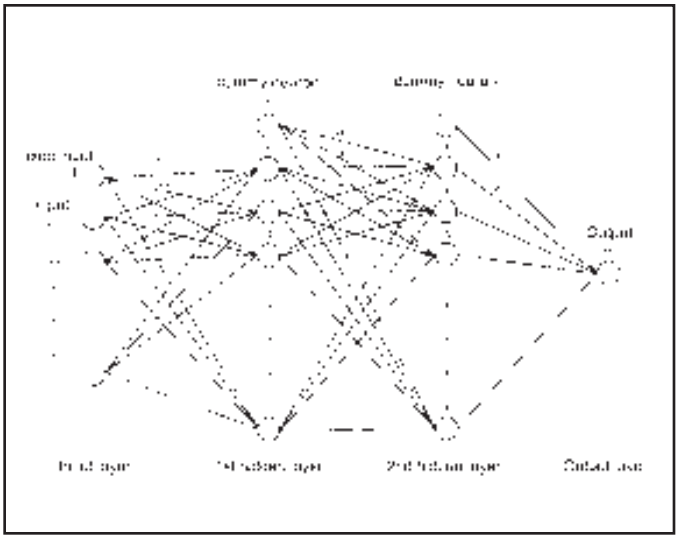

Fig. 3 — Multilayer feed-forward neural network.

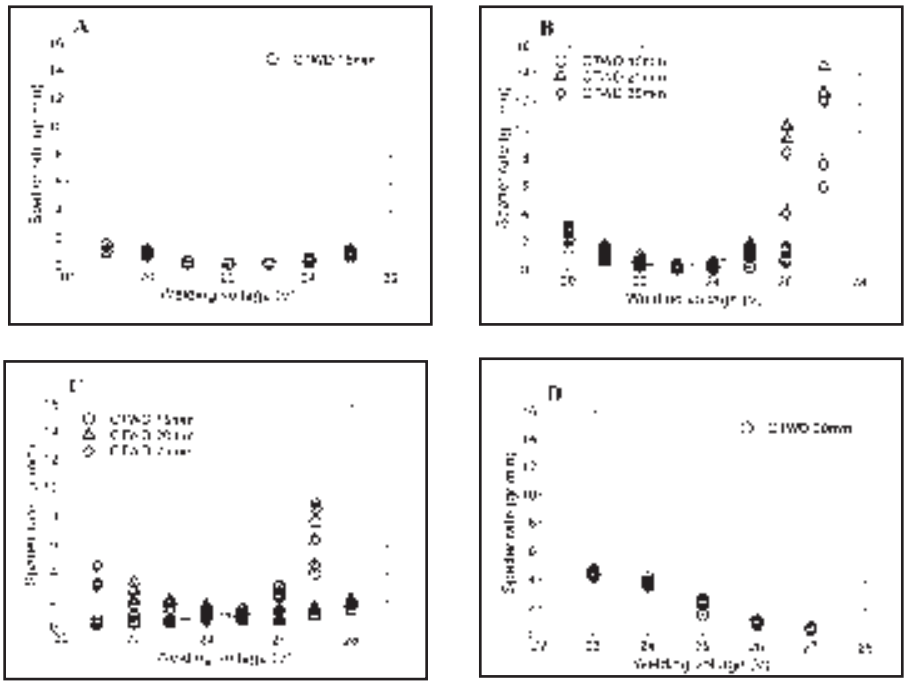

Fig. 4 — The spatter rate with respect to the welding voltage at different wire feed rates. A — Wire feed rate 3.4 m/min; B — wire feed rate 6.0 m/min; C — wire feed rate 7.3 m/min; D — wire feed rate 8.6 m/min.

stantaneous current (I_s), average current during short-circuit period ($\bar{I}$), standard deviation of the short-circuit period ($s[T]$), standard deviation of arc time ($s[T_a]$), standard deviation of short-circuit time ($s[T_s]$), standard deviation of short-circuit peak current ($s[I_p]$), standard deviation of short-circuit instantaneous current ($s[I_s]$), standard deviation of average current during short-circuit period ($s[\bar{I}]$).

Neural Network Structure

The purpose of this study is to develop models for evaluating the spatter rate based on the conventional feed-forward multilayer perceptrons with the error back-propagation as the learning algorithm. The neural network with typical feed-forward multilayer perceptrons is composed of an input layer, hidden layer, and output layer. The neural network structure used in this study is shown in Fig. 3. The variables of the input layer are the aforementioned 12 factors, whereas the output variable is the spatter rate. Of course, there are many other factors, such as power source characteristics, inductance, contact tube-to-workpiece distance (CTWD), shielding gas, and the size and chemical composition of the electrode, affecting the spatter generation in short circuiting metal transfer with GMAW. But since the variation of these factors induces the variation of the welding current and voltage waveform, it is very efficient to use the waveform factors instead of all affecting factors as the input variables of the neural network model for spatter rate estimation. The neural network model was programmed using the C++ program code without using other commercial software packages.

An output of the hidden layer is produced using the values of the input variables and the connection weight. The output of the output layer is obtained by processing the output of the hidden layer and the relevant connection weight, and this process can be expressed as shown in Equations 1–3.

$$y_j = f\left(\sum_{i=0}^{l} v_{ji} z_i\right) \qquad \left(j = 1,2,...,m\right) \tag{1}$$

$$x_t = f\left(\sum_{j=0}^{m} u_{tj} y_j\right) \qquad \left(t = 1,2,...,n\right) \tag{2}$$

$$o = f\left(\sum_{t=0}^{n} w_t x_t\right) \tag{3}$$

Where z_i is the input vector of the input layer, y_j, x_t, and o are the output vectors of the hidden layers and output layer, respectively. v_{ji}, u_{tj}, and w_t are the arrays of connection weight, and l, m, and n are the number of the neurons in the input and hidden layers, respectively. Bipolar sigmoid function was adopted as an activation function in Equation 4 due to its popularity.

$$f(x) = \frac{2}{1+\exp(-x)} - 1 \tag{4}$$

The least square method was used in the error calculation as shown in Equation 5

$$E = \frac{1}{2p} \sum_{k=1}^{p} (d_k - o_k)^2 \tag{5}$$

where E is the cost function measuring the mean squared error and p is the number of learning patterns. d_k is the kth desired value and o_k is the kth output value of the neural network. $2p$ was used in order to normalize the cost function in the range of [0, 1].

The values of the connection weights in the learning process are changed to minimize the mean squared error, E, based on Equations 6 through 8, and thus the values of the connection weights are adjusted to the opposite direction of the gradient of the mean squared error, E, and learning is performed in the direction in which the error decreases. The rate of the decrease depends on the learning rate η.

$$\Delta w_t = -\eta \frac{fE}{fw_t} \tag{6}$$

$$\Delta u_{tj} = -\eta \frac{fE}{fu_{tj}} \tag{7}$$

$$\Delta v_{ji} = -\eta \frac{fE}{fv_{ji}} \tag{8}$$

The Learning Procedure for the Spatter Rate Estimation

A fixed input of –1 was added to the input and hidden layers while the initial number of neurons of each layer was established as $l = 12$, $m = 20$, and $n = 20$ in the learning process for the spatter rate estimation while that of the output layer was 1. The connection weights v_{ji}, u_{tj}, and w_t were expressed in an array with the sizes of $[m \langle (l+1)]$, $[n \langle (m+1)]$, and $[1 \langle (n+1)]$, respectively. These were initialized as the random values between [–1, 1] before learning, and the input vectors, waveform factors in other words, z, were made to have values normalized as –1 to the minimum value and as 1 to the maximum value. In addition, the output vector o, the spatter rate estimated through learning, was normalized to have a value between the range of [–1, 1], and the learning rate was 0.1 and the error boundary was established as 0.002 to the cost function, E, between the estimated results of the normalized output variable and the normalized values to spatter rate.

Optimization of the Neural Network

In constituting the multiple layers neural network model, the number of hidden layers and the number of nodes of each layer may influence the output. The number of hidden layers of the neural network in this study was fixed at two. One hidden layer neural network model retained the divergence problem and a three or more hidden layers model retained the convergent time problem. The three-layer model with two hidden layers, therefore, was determined as optimal in terms of the convergence and convergent time. The number of neurons is also a very important factor for estimation performance. Networks with too few trainable parameters for the given amount of training data fail to learn the training data. With too many trainable parameters, the network learns well but does not generalize well and performs very poorly on the new

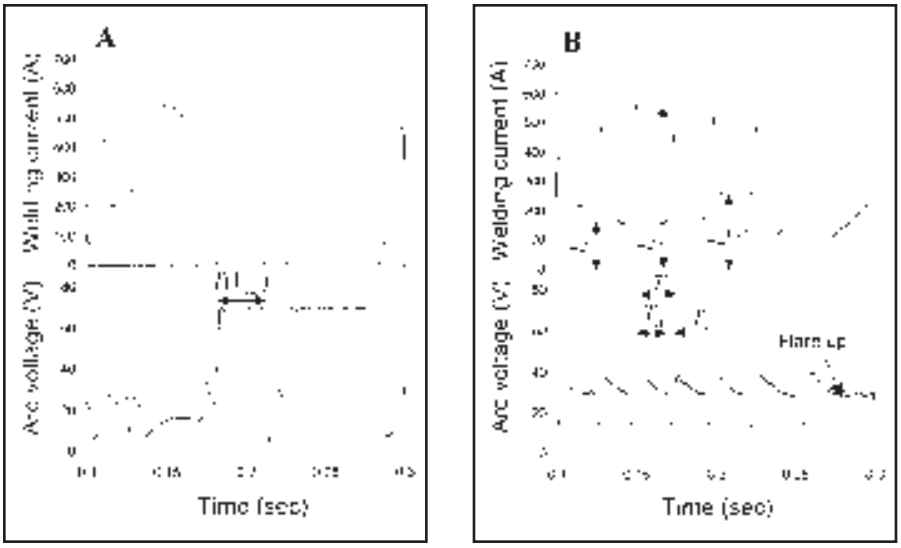

Fig. 5 — Waveforms of the arc voltage and the welding current under the lower and upper welding voltage condition. A — 150 A, 19 V; B — 250 A, 28 V.

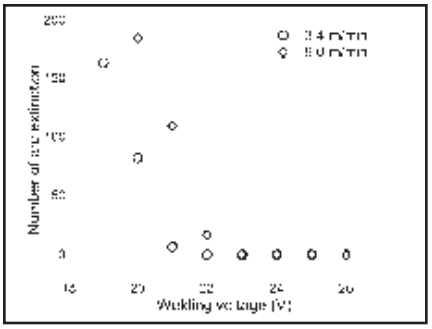

Fig. 6 — Number of arc extinctions with respect to the welding voltages at a CTWD of 15 mm.

Table 2 — Correlation Coefficients between Each Factor and Spatter Rate in the Various Regions

Region	T	T_a	T_s	I_p	I_s	$\bar{I}$	s[T]	s[T_a]	s[T_s]	s[I_p]	s[I_s]	s[$\bar{I}$]
Overall	**0.9198**	**0.723**	–0.109	0.1746	0.2615	–0.163	**0.7457**	**0.7361**	0.1749	0.5019	0.1986	0.0423
Arc extinction	0.0593	0.0437	0.1235	0.230	0.351	–0.006	0.4312	0.3666	**0.6504**	**0.7650**	**0.8886**	**0.8816**
No arc extinction	**0.8165**	**0.8267**	–0.164	0.1757	0.2592	–0.273	**0.7914**	**0.7876**	0.2565	0.6562	0.1398	–0.3033

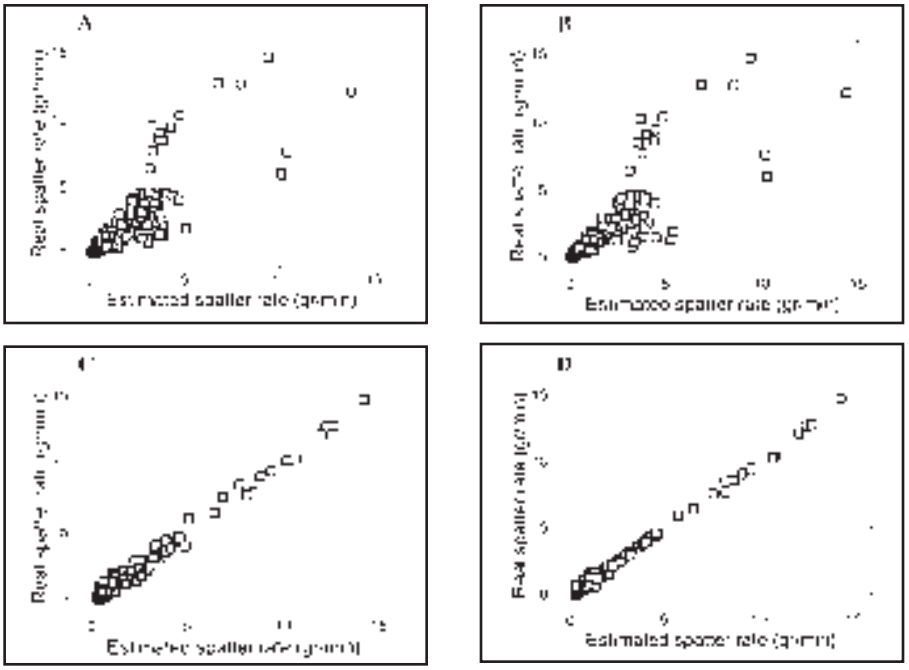

Fig. 7 — Relationship between the estimated results and the spatter rate with the trained data set using several models. A — Nonlinear regression model in overall range; B — combined nonlinear regression model; C — neural network model in overall range; D — combined neural network model.

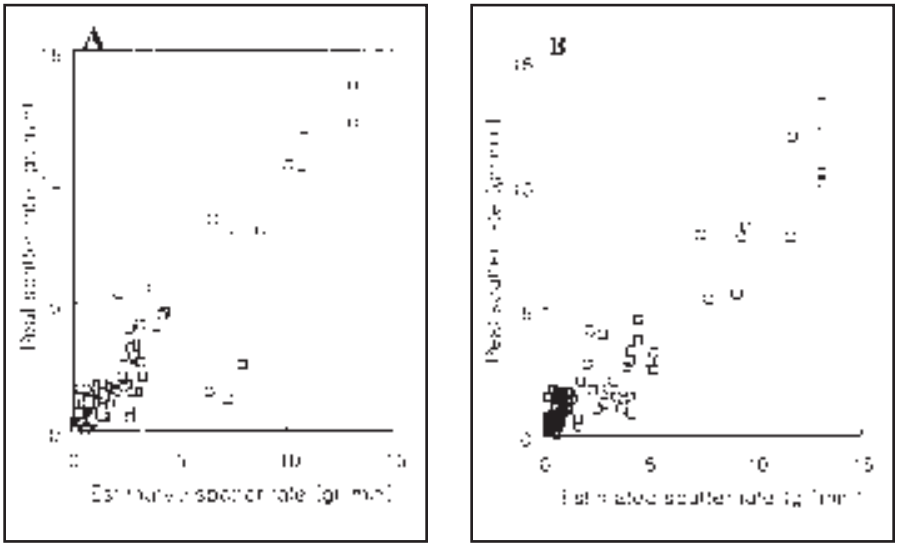

Fig. 8 — Comparison of estimation performance between model of overall range and combined model with a new data set. A — Neural network model in overall range; B — combined neural network model.

Table 3 — Input Variables of Each Neural Network Model

Model	T	T_a	T_s	I_p	I_s	$\bar{I}$	s[T]	s[T_a]	s[T_s]	s[I_p]	s[I_s]	s[$\bar{I}$]
Overall	O	O		O	O		O	O	O	O	O	O
Arc extinction		O	O	O	O			O	O	O	O	O
No arc extinction	O	O		O	O		O	O	O	O	O	

data not used in training. This phenomenon is usually called overfitting (Ref. 13). There are several generalization methods: regularization technique using modified performance function, automated regularization method, early stopping technique, etc. (Ref. 14). One of the generalization methods is to use a network that is just large enough to provide an adequate fit. In this study, by optimizing the number of input and hidden nodes, the optimal-sized neural networks could be obtained. In optimizing the neurons of the input layer, the factors with the lowest correlation coefficients (Table 2) between each variable of the input layer and the spatter rate were removed in turn within the convergence condition of an error boundary of 0.002. In optimizing the neurons of the hidden layers, the number of neurons ($20 \langle 20$) was reduced as long as they converge within the limited number of repetitions (10,000 times).

Results and Discussion

Neural Network Models for the Spatter Rate Estimation

Spatter rate was measured for all the welds using the conditions shown in Table 1. As shown in Fig. 4, there was an optimal voltage wherein the minimum spatter rate was generated.

Figure 5 shows the typical waveforms of the arc voltage and welding current where one is for high current-voltage and the other is for low current-voltage. In Fig. 5A, it can be seen that the arc is reignited after the short circuit and the arc is then completely extinct, showing the open-circuit voltage. This "arc extinction" is different from the arc extinguishment caused by the short circuit where the metal droplet is contacted to the weld pool. This leads to an understanding that the arc extinguishes and the circuit is electrically disconnected at the moment of arc reignition after the short-circuit period. Figure 6 shows the number of arc extinctions generated, not at the moment of short circuit but at the moment of arc reignition. This number was gradually reduced as the welding voltage increased, and the arc extinction subsequently did not occur as the voltage became higher than a certain value.

The correlation analysis between 12 waveform factors and the spatter rate was performed for the three cases as follows: the overall range without considering the arc extinction, the welding conditions wherein the arc extinction occurs, and the welding conditions without the arc extinction. The second row of Table 2 shows the correlation coefficients between the spatter rate and waveform factors obtained under all welding conditions — overall range in other words — regardless of the

arc extinction. The third row shows under welding conditions where arc extinction occurred, while the fourth row shows under welding conditions where the arc extinction did not occur. According to the second and fourth row of Table 2, the behavior of the correlation coefficients in all cases was very similar, and the primary factors affecting the spatter rate, in particular, were the short-circuit period (T), the standard deviation of the short-circuit period ($s[T]$), the standard deviation of the arc time ($s[T_a]$), and arc time (T_a), et al. The two factors, the short-circuit time (T_s) and average current during a short circuit ($\bar{I}$), were eliminated to prevent the multicolinearity. The standard deviation of average current during a short-circuit period ($s[I]$), the standard deviation of short-circuit instantaneous current ($s[I_s]$), the standard deviation of short-circuit peak current ($s[I_p]$), and the standard deviation of short-circuit time ($s[T_s]$), nevertheless, affected the spatter rate to a great extent according to the third row of Table 2. It is shown that the primary waveform factors for the spatter generation when the arc extinction occurs differ from those when the arc extinction does not occur. A model in overall range without considering the arc extinction and another model considering the arc extinction were proposed to develop a more precise model for the spatter rate estimation and to compare the estimation performance. The model considering the arc extinction combines two conditions: one under welding conditions where the arc extinction occurs and the other where it does not occur.

The Neural Network Model for the Spatter Rate Estimation in the Overall Range

The hidden layer was first set at 20 ⟨ 20, and the number of neurons of the hidden layer was reduced in turn as long as they converge within 10,000 repetitions, in developing the neural network model for the spatter rate estimation in the overall range. Finally, the size of neurons in the hidden layer of 5 ⟨ 5 with an error of 0.00196 was obtained in 9976 repetitions. The 12 waveform factors were then gradually eliminated in optimizing the input variables, beginning with those with the lowest correlation coefficient on the spatter rate based on the correlation analysis of Table 2. Last, the input variables remaining within the convergence error bound during 10,000 repetitions were the 10 factors in Table 3.

The Neural Network Model for the Spatter Rate Estimation Considering Arc Extinction

In welding conditions where the arc extinction occurs, it was confirmed that the hidden layer of the neural network model for estimating the spatter rate was optimized to a size of 7 ⟨ 5 in 9983 repetitions with a normalized output error of 0.00199. The input variables were optimized based on the results of the correlation analysis in Table 2. As a result, the factors of the input layer were the nine factors in Table 3.

In welding conditions wherein there is no arc extinction, the normalized output

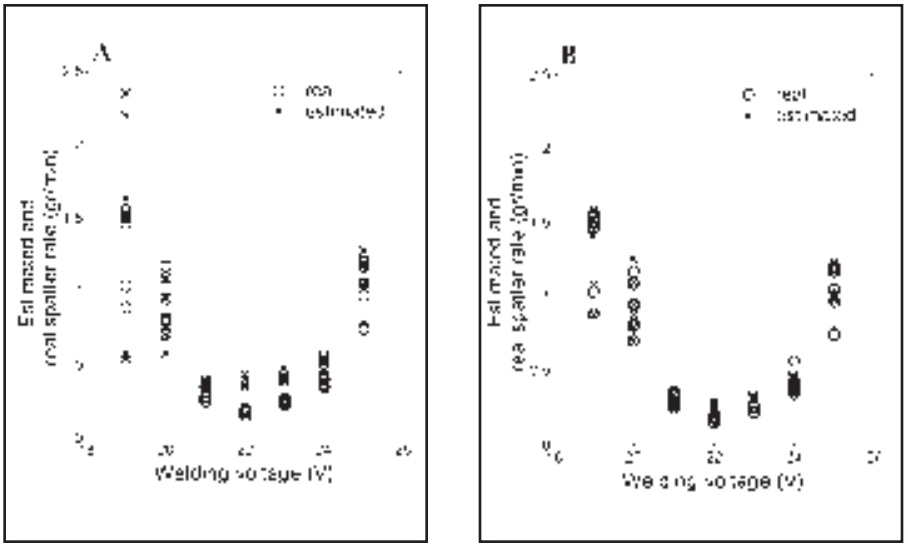

Fig. 9 — Comparison of the estimated results by model in the overall range and combined model with spatter rate (wire feed rate of 3.4 m/min). A — Model in overall range; B — combined model.

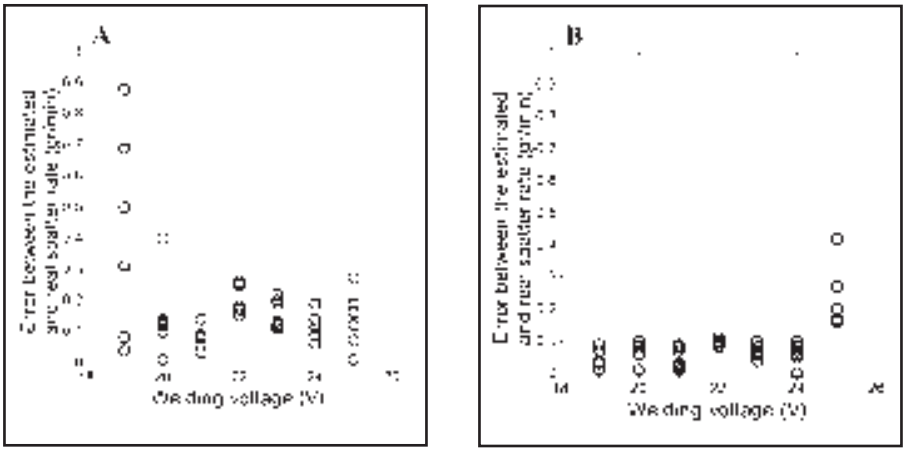

Fig. 10 — Error between the estimated results from model in the overall range and combined model with spatter rate (wire feed rate of 3.4 m/min). A — Model in overall range; B — combined model.

Table 4 — Regression Characteristics of Several Estimation Models

	Nonlinear Regression Model		Neural Network Model			
			Model in Overall Range		Combined Model	
	Model in Overall Range	Combined Model	Trained Data Set	New Data Set	Trained Data Set	New Data Set
Multiple correlation coefficients	0.9109	0.8424	0.9441	0.9156	0.9986	0.9467
Adjusted R^2	0.8258	0.7084	0.9058	0.8368	0.9965	0.8953
Standard error	0.4562	1.2954	0.3134	1.109	0.0691	0.8884

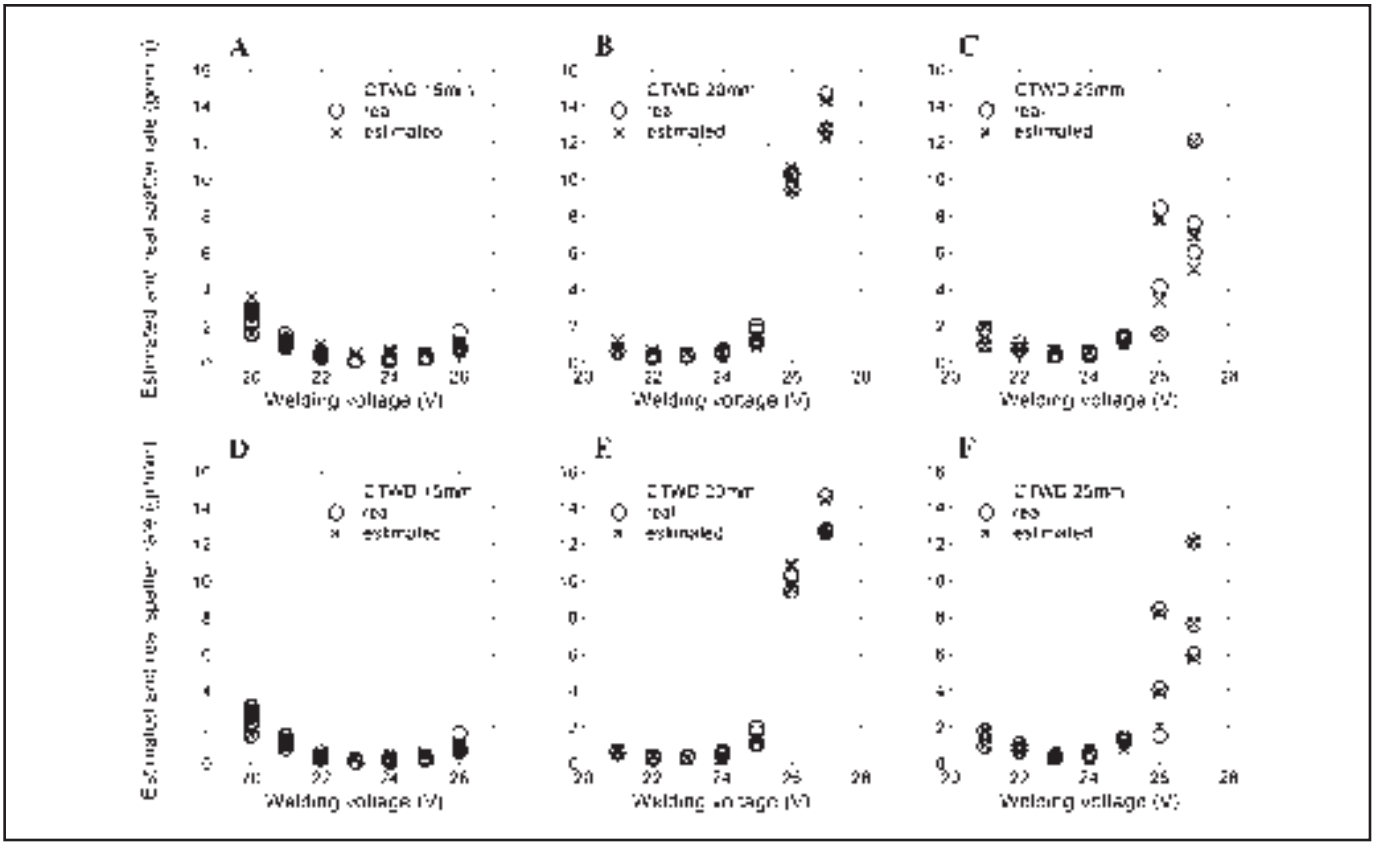

Fig. 11 — Comparison of the estimated results from model in overall range and combined model with spatter rate (wire feed rate of 6.0 m/min). A, B, and C — Model in overall range; D, E, and F — combined model.

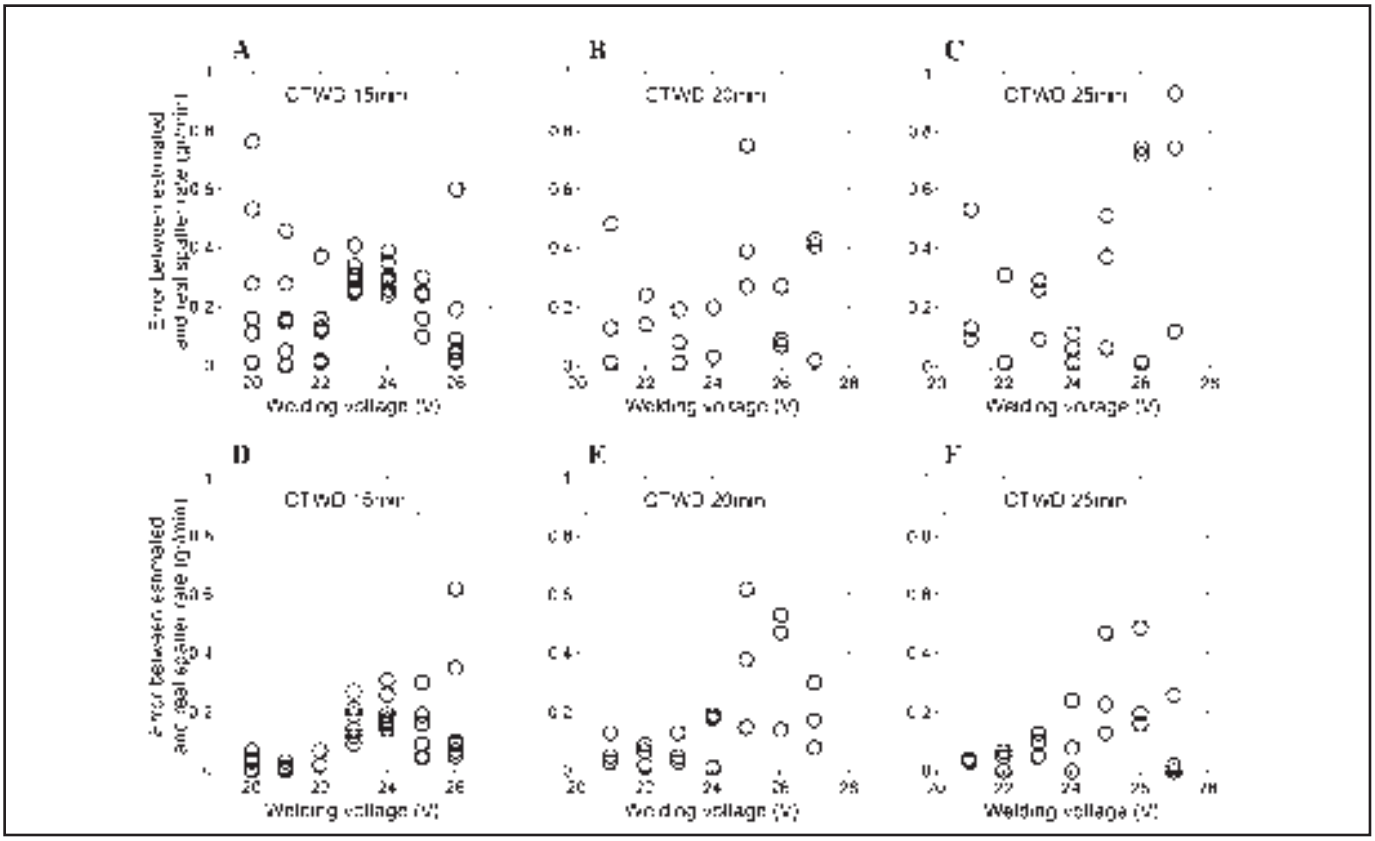

Fig. 12 — Error between the estimated results from model in overall range and combined model with spatter rate (wire feed rate of 6.0 m/min). A, B, and C — Model in overall range; D, E, and F — combined model.

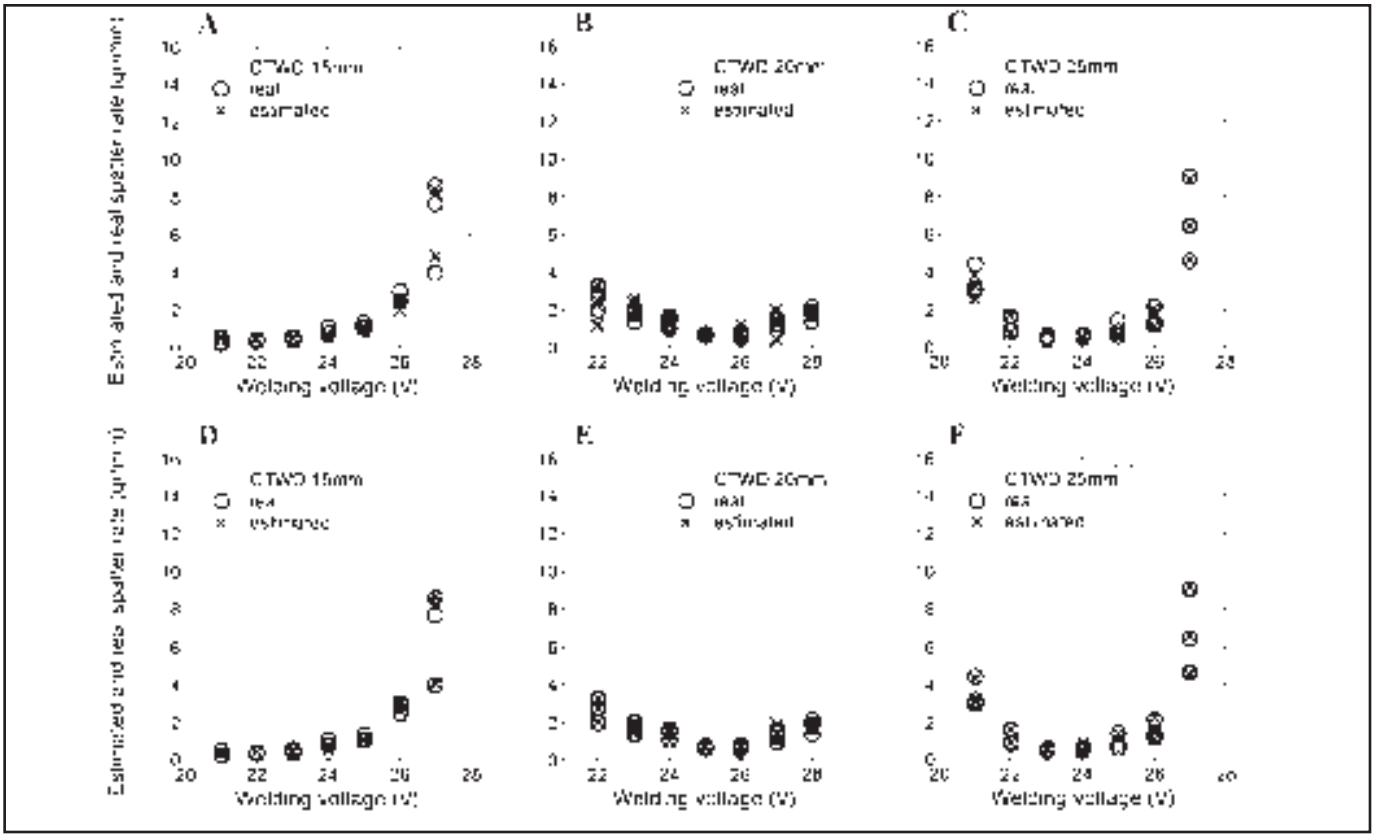

Fig. 13 — Comparison of the estimated results from the model in the overall range and the combined model with spatter rate (wire feed rate of 7.3 m/min). A, B, and C — Model in overall range; D, E, and F — combined model.

error was 0.00198 in 9994 repetitions when the hidden layer was 5 〈 5 in size. The waveform factors were optimized based on the results of the correlation analysis shown in Table 2. As a result, the factors of the input layer were determined as the nine factors in Table 3.

The combined neural network model itself cannot distinguish whether arc extinction occurs or not. The neural network model for the arc extinction region is applied when the arc voltage retains the open circuit voltage value, the occurrence of the arc extinction in other words, and the model for nonarc extinction region is applied otherwise.

Experimental Results

The proposed models were tested using two data sets. One was the trained data set shown in Table 1 and the other was a new set of 108 data. Figure 7 is the tested result with the trained data set. Figure 7A and B shows the estimated results obtained using the overall and combined nonlinear regression models proposed by Kang and Rhee (Ref. 12). Figure 7C and D shows the results of the estimated spatter rate using the neural network models proposed in this study.

A large error was shown in predicting the spatter rate in the regression models. The results with the neural network models, in contrast, were linearly related to the actual spatter rate in ranges where the spatter rate was over 5 g/min, in particular. The estimated results with the neural network model in the overall ranges, nevertheless, retained a slightly larger error rate than that with the combined neural network model in ranges where the spatter rate was under 5 g/min. Figure 8 is the tested result with a new set of 108 data. It could be seen that the dispersion of the estimated results with the combined neural network model was less than that with the neural network model in the overall range.

Table 4 shows the compared results between the regression models and the neural network models, and the multiple regression coefficients obtained using regression models show significantly lower values than those obtained using two neural network models. The multiple correlation coefficients obtained using the combined neural network model show results close to 1, and the standard error with the combined neural network model was determined to be 0.0691, showing a good estimation performance.

When the wire feed rate was set at 3.4 m/min, the estimated results with the neural network model in overall range with the combined model was compared to the spatter rate according to the changes in welding voltage as shown in Fig. 9. As a result, the estimated results of the combined model were considered more accurate than the results of the model in the overall range. The error between the estimated values for each model and the spatter rate to compare the results more accurately is shown in Fig. 10. According to Fig. 10, the estimation error with the neural network model in the overall range is larger than that with the combined model. The estimation error with the combined model was below 0.1 g/min, in particular, under lower voltage welding conditions where the arc extinction occurs, confirming the superiority of the combined model's estimation performance.

Figure 11 shows the estimated results with the neural network model in the overall range and the estimated results with the combined model according to the changes in welding voltage when the wire feed rate is 6 m/min. Figure 12, in addition, shows the estimation error with each model, and the error with the model in the overall range shows the maximum value of 0.78 g/min at CTWD of 15 mm and welding voltage of 19 V, where arc extinction frequently occurs, whereas the estimation error with the combined model was below 0.1 g/min. The estimation error with the model in the overall range at CTWD of 25 mm and the welding voltage of 27 V was

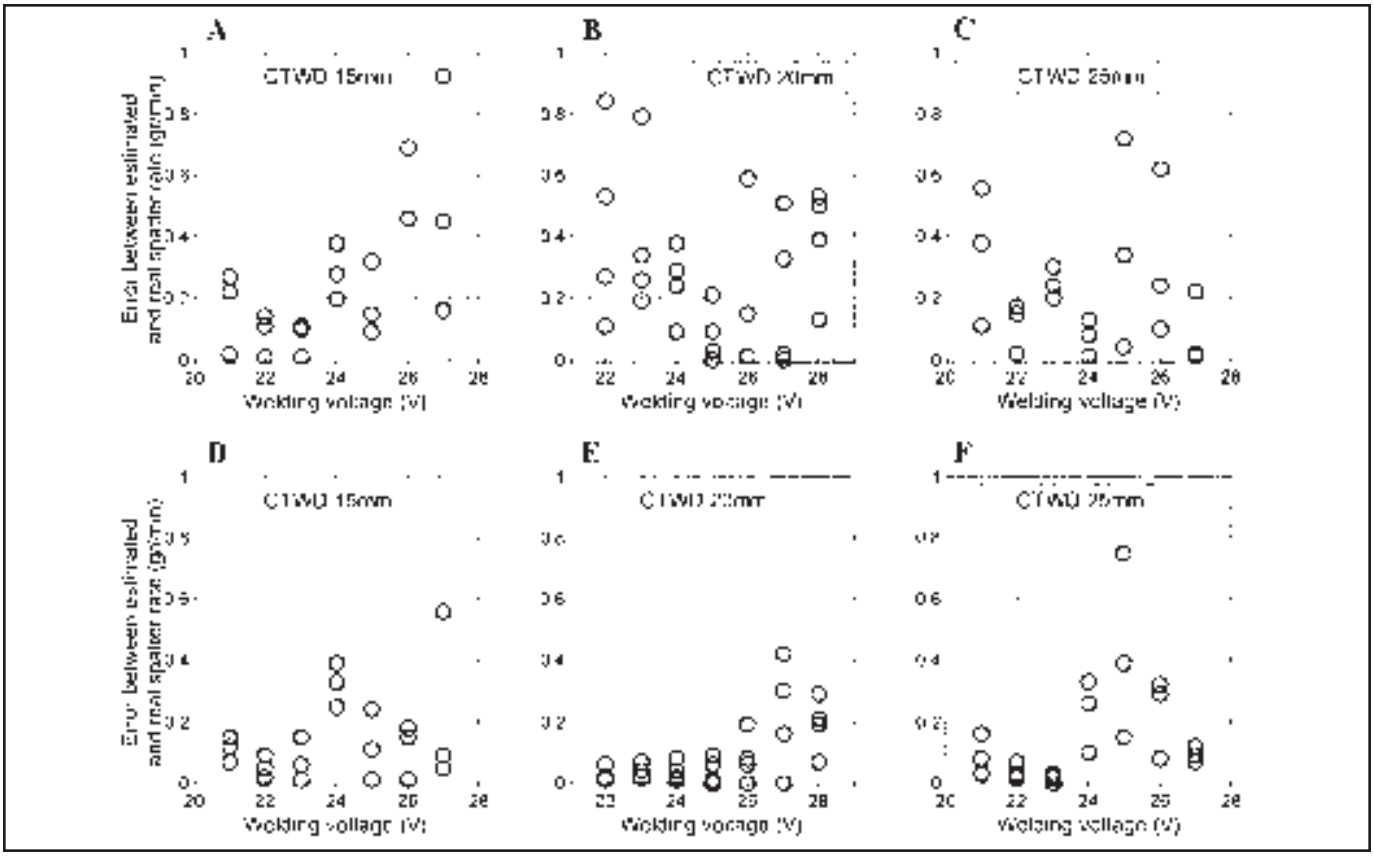

Fig. 14 — Error between the estimated results by model in the overall range and the combined model with spatter rate (wire feed rate of 7.3 m/min). A, B, and C — Model in overall range; D, E, and F — combined model.

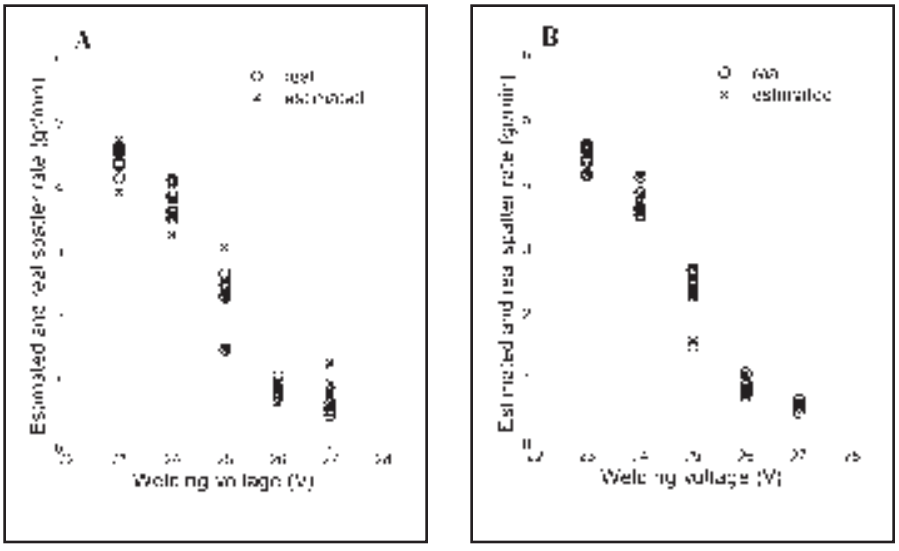

Fig. 15 — Comparison of the estimated results from the model in the overall range and the combined model with spatter rate (wire feed rate of 8.6 m/min). A — Model in overall range; B — combined model.

above the optimal voltage and over 0.9 g/min, while the estimation error with the combined model was below 0.3 g/min. In addition, the estimation errors in the ranges where the arc extinction occurs and the combined model retained an error below 0.2 g/min and an average error below 0.4 g/min under the welding conditions of 25~27 V.

Figure 13 shows the estimated results with the neural network model in the overall range and the estimated results with the combined model when the wire feed rate is 7.3 m/min, according to the changes in the welding voltage, and Fig. 14 shows the estimation error with each model. In CTWD of 20 mm, 25 mm, and lower voltage conditions, where the arc extinction frequently occurs, the estimation error with the model in the overall range retained a maximum estimation error of more than 0.8 g/min. The estimation error with the combined model, on the contrary, shows a value below 0.1 g/min under the low voltage conditions where arc extinction frequently occurs. Furthermore, the estimation error with the combined model was considered better than that with the model in the overall range even in the higher voltage conditions where there is a high spatter rate.

Figure 15 shows the estimated results with the neural network model in the overall range and the estimated results with the combined model when the wire feed rate is 8.6 m/min, according to the changes in the welding voltage. Figure 16 shows the estimation error with each model. The estimation error with the model in the overall range showed the maximum value of 0.3 ~ 0.7 g/min, depending on the voltage condition. The error with the combined model, nevertheless, showed a value below 0.2 g/min over all voltage conditions.

This study confirmed that the combined neural network model where arc extinction was considered demonstrated the ideal estimation performance in the short circuit transfer mode of GMA welding.

Conclusions

A neural network model for the overall range and a combined neural network model that considered arc extinction are proposed in this study. The neural network structure for each model was optimized as [10⟨ 5⟨ 5⟨ 1] and [9⟨ 7⟨ 5⟨ 1] or [9⟨ 5⟨ 5⟨ 1], respectively. As a result, the generalization of the neural network was accomplished and the proposed models were determined to be ideal for the spatter rate estimation compared with the previously proposed results. The combined neural network model, which takes into consideration the arc extinction, showed a linear correlation coefficient of 0.9986 and a standard error of 6.91% regarding the spatter rate. A significant improvement in estimation performance at a lower voltage was demonstrated in this study where arc extinction occurs.

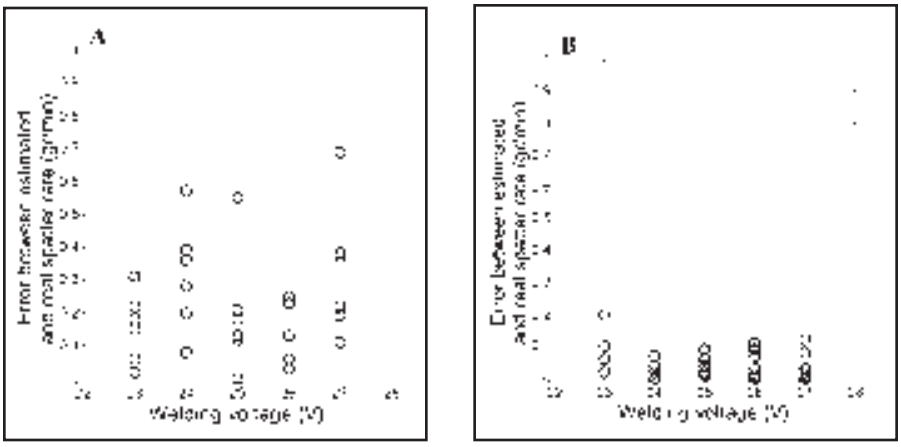

Fig. 16 — Error between the estimated results from the model in the overall range and the combined model with spatter rate (wire feed rate of 8.6 m/min). A — Model in overall range; B — combined model.

References

1. Gupta, S. R., Gupta, P. C., and Rehfeldt, D. 1988. Process stability and spatter generation during dip-transfer MAG-welding. *Welding Review*, pp. 232–241.

2. Arai, T., Kobayashi, M., Yamada, T., Rokujyo, M., Hirakoso, K., and Kaneko, T. 1983. The investigation of arc phenomena by means of a computer. *Quarterly Journal of the Japan Welding Society* 1(3): 15–20.

3. Lucas, W. 1987 : Microcomputer system, Software and expert system for welding engineering, *Welding Journal* 66(4): 19–30.

4. Suban, M. 2001. Determination of stability of MIG/MAG welding. *Quality and Reliability Engineering International* 17: 345–353.

5. Shinoda, T., and Nishikawa, H. 1995. Monitoring and signal processing of short circuiting metal transfer of metal active gas welding process. *Proc. of the Int. Conf. on the Joining of Materials, JOM-7*, pp. 558–565. Helsingor, Denmark: The European Institute for the Joining of Materials.

6. Gupta, S. R., and Gupta, P. C. 1984. Effect of some variables on spatter loss. *Welding and Metal Fabrication* 52(9): 361–364.

7. Hermans, M. J. M., Sipkes, M. P., and Ouden, G. D. 1993. Characteristic features of the short circuiting arc welding process. *Welding Review International* 12(2): 80–86.

8. Hermans, M. J. M., and Ouden, G. D. 1999. Process behavior and stability in short circuit gas metal arc welding. *Welding Journal* 78(4): 137-s to 141-s.

9. Ogunbiyi, B., and Norrish, J. 1996. GMAW metal transfer and arc stability assessment using monitoring indices. *Computer Technology in Welding, Sixth International Conference.* Cambridge, U.K.: The Welding Institute.

10. Mita, T., Sakabe, A., and Yokoo, T. 1988. Quantitative estimates of arc stability for CO_2 gas shielded arc welding. *Welding International* 2(2): 152–159.

11. Kang, M. J., and Rhee, S. 2001. A study on the development of the arc stability index using multiple regression analysis in the short circuit transfer region of gas metal arc welding. *Proc. Inst. Mech. Engrs. Part B* 215: 195–205.

12. Kang, M. J., and Rhee, S. 2001. The statistical models for estimating the spatter rate in the short circuit transfer mode of GMAW. *Welding Journal* 80(1): 1-s to 8-s.

13. Lin, C. T., and Lee, C. S., George. 1996. *Neural Fuzzy Systems: A Neuro-Fuzzy Synergism to Intelligent Systems*, Upper Saddle River, N.J.: Prentice Hall.

14. Demuth, H. B., and Beale, M. H. 1997. *Neural Network Toolbox.* Miami, Fla.: The MathWorks.

2004 Poster Session
Call for Entries

The American Welding Society announces a Call for Entries for the 2004 Poster Session to be held as part of Welding Show 2004 on April 6-8, 2004, in Chicago, Ill. Students, educators, researchers, engineers, technical committees, consultants, and anyone else in a welding- or joining-related field are invited to participate in the world's leading annual welding event by visually displaying their technical accomplishments in a brief graphic presentation, suitable for close, first-hand examination by interested individuals.

Posters provide an ideal format to present results that are best communicated visually, more suited for display than verbal presentation before a large audience; new techniques or procedures that are best discussed in detail individually with interested viewers; brief reports on work in progress; and results that call for the close study of photomicrographs or other illustrative materials.

Submissions should fall into one of the following two categories and will be accepted only in a specific format. Individuals interested in participating should contact Dorcas Troche, Manager, Conferences & Seminars, via e-mail at dorcas@aws.org for specific details. Deadline for submission of entries is Monday, December 1, 2003.

1. Student Division
   - ∞Category A: 2 Year or Certificate Program
   - ∞Category B: Undergraduate Degree
   - ∞Category C: Graduate Degree

2. Professional/Commercial Divison